Optimized pupil-plane filters for confocal microscope point-spread function engineering

M. A. A. Neil, R. Juškaitis, T. Wilson, and Z. J. Laczik

Department of Engineering Science, University of Oxford, Parks Road, Oxford OX1 3PJ, UK

V. Sarafis

Centre for Microscopy and Microanalysis, University of Queensland, Brisbane, Queensland 4072, Australia

Received October 27, 1999

We present a new method of superresolving pupil-plane filter design in confocal microscopy in which we specify the properties of the desired point-spread function and use an optimization procedure to determine a suitable pupil-plane filter. A new, flexible method of filter implementation using reconfigurable binary optical elements is described, and experimental results are presented. © 2000 Optical Society of America

OCIS codes: 170.1790, 120.2440.

Although the confocal optical system is most frequently employed in the imaging of three-dimensional objects, it is important to remember that in addition to its unique optical sectioning property this system also exhibits enhanced lateral resolution over that which can be obtained with a conventional microscope.[1,2] In essence the confocal optical system may be regarded as a coherent optical processor with an effective amplitude point-spread function given by the product of the amplitude point-spread functions of the two imaging lenses. It is this property that has encouraged many researchers to contemplate achieving superresolution by introducing suitable pupil-plane filters into the optical system.[3–6] Although such filters can be designed to give a narrower central lobe to the point-spread function of the objective lens, this is often at the expense of enhanced sidelobe levels. However, the multiplicative nature of the effective point-spread function of the confocal system provides one with the opportunity to reduce the sidelobe levels to produce an acceptable overall point-spread function. The traditional approach to producing a superresolving point-spread function has been to begin by selecting a particular form for the pupil-function mask. A number of free parameters are then chosen to give, say, a particular position for the first zero in the focal-plane distribution, together with an acceptable sidelobe level. In this Letter we introduce an alternative design philosophy that enables us to specify directly the properties that the final effective pupil function should possess. We also describe a new method by which such filters can be implemented in a confocal microscope.

We begin by specifying the properties that we wish the final effective point-spread function to have and then use an optimization technique to determine an appropriate pupil-function filter. We make no initial assumptions as to the form of pupil-function filter. This form is produced directly by the optimization algorithm. Of course there may not be an exact solution to the specification, but this method does have the advantage that it allows one to find a solution that matches the important aspects of the desired result as closely as possible. To illustrate our new approach we restrict our attention to a reflection-geometry confocal microscope, although the approach is equally valid in single- and multiple-photon fluorescence systems. We first assume that a pupil-modifying filter is employed in only one of the imaging objectives. The pupil of the other objective is clear and unapodized. The overall intensity point-spread function of the system can be written as

$$I(t, w, u) = |h_i(t, w, u)h_d(t, w, u)|^2, \tag{1}$$

where the lateral optical coordinate t is related to the actual lateral distance, x, by $t = (2\pi/\lambda)x \sin\alpha$, where λ denotes the wavelength and $\sin\alpha$ the numerical aperture. A similar expression relates w to y, whereas the axial optical coordinate, u, is related to the actual axial distance, z, by $u = (8\pi/\lambda)z \sin^2(\alpha/2)$. The amplitude point-spread functions, $h_{i,d}$, are related to the pupil functions, $P_{i,d}$, by[1]

$$h_{i,d}(t, w, u) = \iint_P P_{i,d}(\xi, \eta)\exp\left[-\frac{1}{2} ju(\xi^2 + \eta^2)\right] \times \exp[-j(\xi t + \eta w)]\mathrm{d}\xi\mathrm{d}\eta\,, \tag{2}$$

where P_i is the illumination pupil and P_d is the detection pupil. Here we choose an unapodized clear detection pupil such that $P_d(\xi, \eta) = 1; (\xi^2 + \eta^2)^{1/2} < 1$. The form of the apodized illumination pupil, on the other hand, is chosen as a result of the optimization procedure. Of course, we can interchange these two pupils to achieve an identical result, although when the apodized pupil modifies the intensity it would be advantageous to place it in the illumination path of a fluorescence microscope.

To provide a concrete example of our approach we shall initially limit out attention to real, binary, phase-only, pupil-plane filters; i.e., the amplitude transmissivity of the filters is restricted to be either $+1$ or -1. We then use a direct binary search algorithm to produce a filter to minimize the least-squares error between the intensities at specified points in the desired intensity point-spread function and those in the actual point-spread function.[7,8] Thus, for example, we might try to design a filter that has an effective intensity point-spread function that is laterally

0146-9592/00/040245-03$15.00/0

85% of the width of the normal unapodized case. In this case our desired relative target values would be $I(0, 0, 0) = 1.0$, together with $I(0.85\nu_0, 0, 0) = 0.5$ and $I(0, 0.85\nu_0, 0) = 0.5$, where $\nu_0 = 1.16$ optical units is the half-width in the unapodized case. We prefer to specify a desired half-width rather than the specific positions of any zeros, since the half-width is likely to be more important in practice. We emphasize that these three values are the only targets that we specify in the direct binary search algorithm. The algorithm then computes a real, phase-only, filter that we implement in our confocal microscope, using the optical system shown in Fig. 1.

Instead of implementing our filter designs by use of physical filters, we prefer to use a technique with a reconfigurable binary optical element[9,10] that, apart from its ease of implementation, allows rapid switching among any number of predesigned filters. The heart of the system is a ferroelectric liquid-crystal spatial light modulator whose individual pixels can exhibit an amplitude reflectivity of $+1$ or -1. The pixels are configured so that when the spatial light modulator is positioned in the input plane of a 4-f optical system one can use a spatial filter (pinhole) in the Fourier plane to filter out a particular diffracted order. This order, when it is retransformed by the second lens, produces the desired (complex) wave front,[9,10] which is then projected onto the back focal plane of the objective lens.

Figure 2 shows the forms of a number of filters, together with experimentally measured $x-z$ sections of the corresponding confocal intensity point-spread functions. The images were taken in a mechanically scanning confocal microscope with 532-nm illumination from a frequency-doubled Nd:YAG laser together with a Leica 1.4-N.A. oil-immersion objective lens. We stopped the aperture of the lens down to unity N.A. to ensure aberration-free performance. A 100-nm gold bead was used as a point object. The top row of Fig. 2 shows the usual case of a confocal microscope with two clear, unapodized pupil functions. The second row shows the result of designing a filter to give axial resolution that is 85% of that in the clear case (Z85). In this case the target values given to the optimization procedure were merely $I(0, 0, 0) = 1.0$, together with $I(0, 0, 0.85u_0) = 0.5$, where $u_0 = 4$ optical units is the half-width in the clear, unapodized case. It can be seen that we have achieved this improvement quite successfully without compromising the lateral resolution or causing unduly high sidelobe levels. If one attempts to further improve the axial resolution, say to 75%, then it becomes clear (Z75) that this is at the expense of a slight reduction in lateral resolution and increased axial sidelobe levels. If we now attempt to improve the lateral resolution to 85% of the clear, unapodized value, then, as we have said, three target values must be provided to the optimizer. The results are shown in Fig. 2 as X85, in which it can be seen that the improvement laterally is at the expense of axial performance. Finally, an attempt to improve both the lateral and axial resolution to 90% of their unapodized values is shown as XZ90. Attempts to reduce the half-width significantly from 90% resulted in unacceptable sidelobe levels. We show in Fig. 3 axial and lateral sections through the experimental point-spread functions for the various filters. Although in each case we have normalized the intensity at the focal point, $I(0, 0, 0)$, to be unity for ease of comparison, it is important to realize that this value depends on the actual filter that is used. Relative to the clear, unapodized case, the four filters have the following focal-point intensities: 27% (Z85), 11% (Z75), 20% (X85), and 10% (XZ90). However, it has to be remembered that the total amount of light projected onto the sample remains the same when pure-phase filters are used and therefore that the sample bleaches at the same rate as in the unapodized case. In all these examples we note that

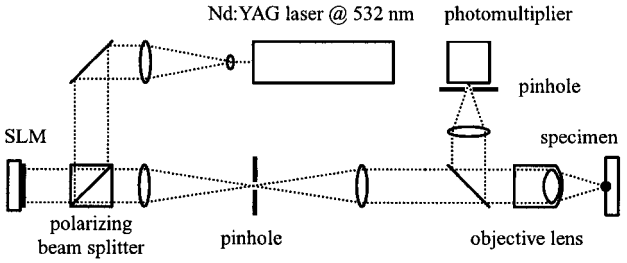

Fig. 1. Schematic diagram of the optical system of the confocal microscope, together with the system used to create the pupil-plane filter. SLM, spatial light modulator.

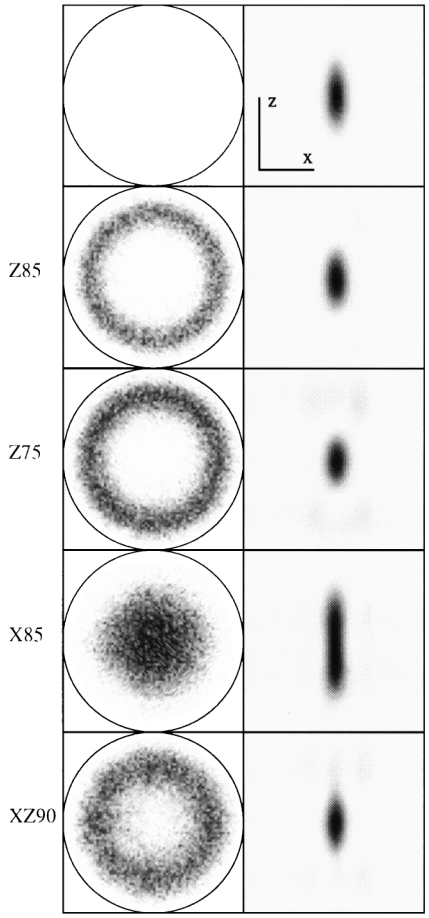

Fig. 2. Pupil-plane phase distribution (left-hand column) together with experimental $x-z$ sections (right-hand column) of the corresponding confocal intensity point-spread functions for the filters described in the text.

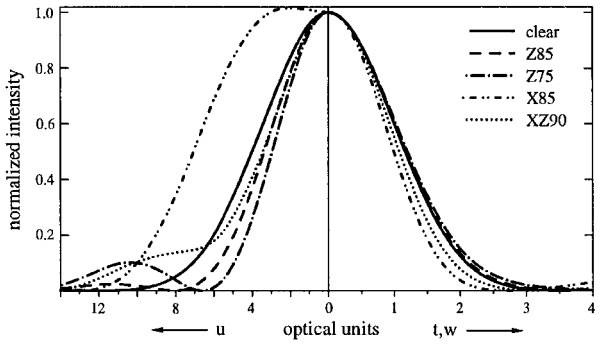

Fig. 3. Axial (left-hand side) and lateral (right-hand side) sections through the experimental point-spread functions of Fig. 2.

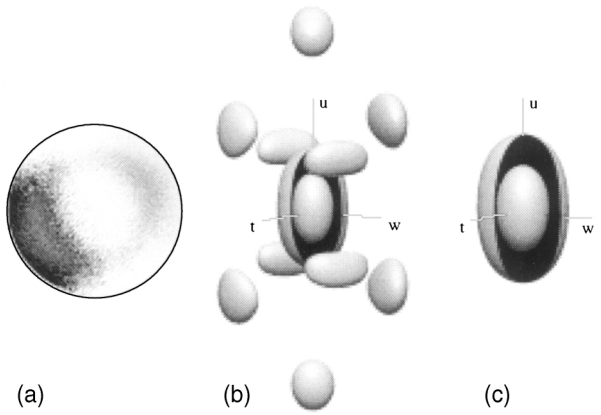

Fig. 4. Results of optimizing for both illumination and detection pupil functions to achieve a reduction in the lateral and the axial half-widths to 80% of the unapodized case: (a) pupil-plane phase filter, $P_i = P_d{}^*$. Also shown are 10% and 50% isosurfaces for the (b) apodized and (c) unapodized intensity point-spread functions.

the optimization procedure produces noisy filters. In fact, this can be considered as the algorithm's finding a dithered solution that mimics amplitude as well as phase modulation in the pupil plane.

We have so far considered only the case in which an apodizing filter is used in one of the objective lenses. There is, of course, no reason not to use (different) filters in both pupils, and the optimization algorithm can easily be modified to accommodate this. Initial trials in which we designed pairs of filters with as many as 16 levels of phase each, where only the lateral resolution was considered in the target, invariably led to designs that had one clear aperture and one apodized but purely real aperture; i.e., to the same results as those reported above. However, if one specifies targets outside the focal plane, for example, to improve the axial resolution as well, then multiple-phase-level pupil-plane masks result. Indeed, if we deliberately choose a target that specifies improved and symmetrical axial and lateral resolution, then the optimization procedure converges on solutions of the form $P_i(\xi, \eta) = P_i{}^*(-\xi, -\eta) = P_d{}^*(\xi, \eta)$. If we now apply this rule as a constraint to the optimization procedure, we can ensure that the resulting point-spread function is symmetrical according to $I(t, w, u) = I(t, w, -u) = I(-t, -w, u) = I(-t, -w, -u)$. We note that this symmetry was exploited previously,[11] although in that case the pupil functions that were analyzed were restricted to simple annuli.

Figure 4(a) shows a filter $P_i = P_d{}^*$ designed in this way, where we specify the targets to reduce the axial and the lateral half-widths to 80%. The filters have eight phase levels in 45° steps. Three-dimensional isosurface contour plots of the resulting point-spread function [Fig. 4(b)] show the 10% contour level cut away to reveal the 50% contour level. For comparison, the same contours are plotted for the unapodized case in Fig. 4(c). These results clearly demonstrate a reduction in focal-spot volume to 53% as defined by the 50% contour and also reveal the inevitably higher sidelobes than the unapodized case. The peak sidelobe level is 15% of the on-axis intensity in the apodized case, which itself is only 4.4% of that in the unapodized case.

In conclusion, we have introduced a new paradigm in point-spread function engineering in which we specify the desired result and use an optimization procedure to determine a suitable pupil-plane filter. In particular, our method does not impose any restrictions on the final form of the pupil-function filter, and hence we consider the resulting pupil functions to be close to optimal. Our examples have been specifically concerned with reflected light imaging, although the results apply equally to the fluorescence case, with equal excitation and emission wavelength, and can readily be extended to other imaging modalities. We have also introduced a new and flexible method of implementing such filters in confocal systems.

This work was supported by the Biotechnology and Biological Sciences Research Council (UK). Z. J. Luczik acknowledges support from the Royal Society of London. T. Wilson's e-mail address is tony.wilson@eng.ox.ac.uk.

References

1. T. Wilson and C. J. R. Sheppard, *Theory and Practice of Scanning Optical Microscopy* (Academic, London, 1984).
2. T. Wilson, ed., *Confocal Microscopy* (Academic, London, 1990).
3. Z. Hegedus, Opt. Acta **32,** 815 (1985).
4. Z. Hegedus and V. Sarafis, J. Opt. Soc. Am. A **3,** 1892 (1986).
5. T. Wilson and S. J. Hewlett, Opt. Lett. **16,** 1062 (1991).
6. M. Martinez-Corral, P. Andres, C. J. Zapata-Rodriguez, and M. Kowalczyk, Opt. Commun. **165,** 267 (1999).
7. M. A. Seldowitz, J. P. Allebach, and D. W. Sweeney, Appl. Opt. **26,** 2788 (1987).
8. H. Y. Chen, N. Mayhew, E. G. S. Paige, and G. G. Yang, Microelectron. Eng. **30,** 95 (1996).
9. M. A. A. Neil, M. J. Booth, and T. Wilson, Opt. Lett. **23,** 1841 (1998).
10. M. A. A. Neil, T. Wilson, and R. Juškaitis, "A wavefront generator for complex pupil function synthesis and point spread function engineering," J. Microsc. (to be published).
11. M. Kowalczyk, C. J. Zapata-Rodriguez, and M. Martinez-Corral, Appl. Opt. **37,** 8206 (1998).